CALIBRATION

- Performance of calorimeters determined by processes that take place in the last stages of the shower development (MeV/keV/eV level)

- This has important consequences for calibration of *longitudinally segmented* devices

- The sampling fraction is a function of *depth* (or shower *age*).
  Example: in em showers, soft γs are sampled differently than mips.
  $\rightarrow$ Ratio (energy deposit/resulting signal) is function of depth.
  Effect is *energy dependent* as well.

The sampling fraction changes with depth!

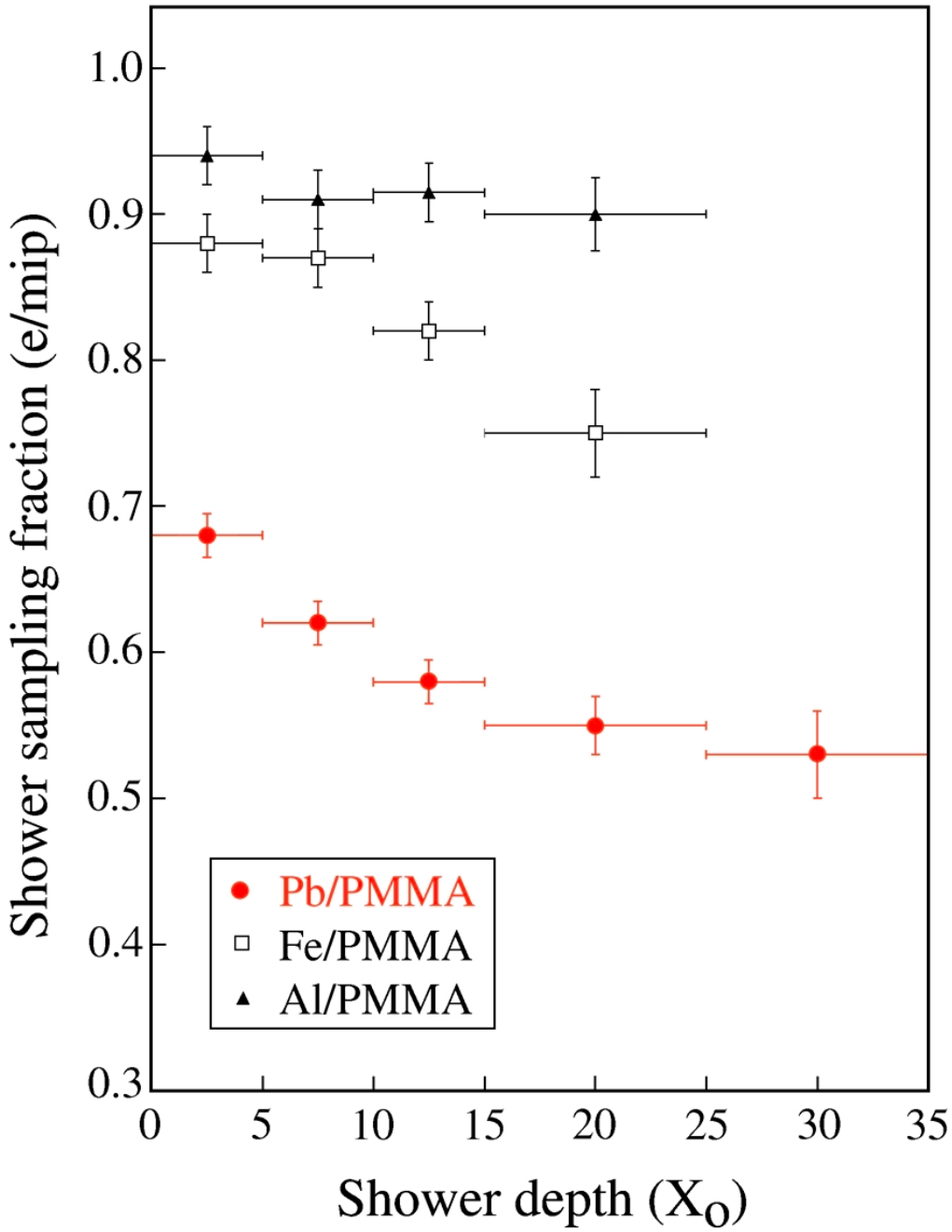

Effects of depth dependence sampling fraction

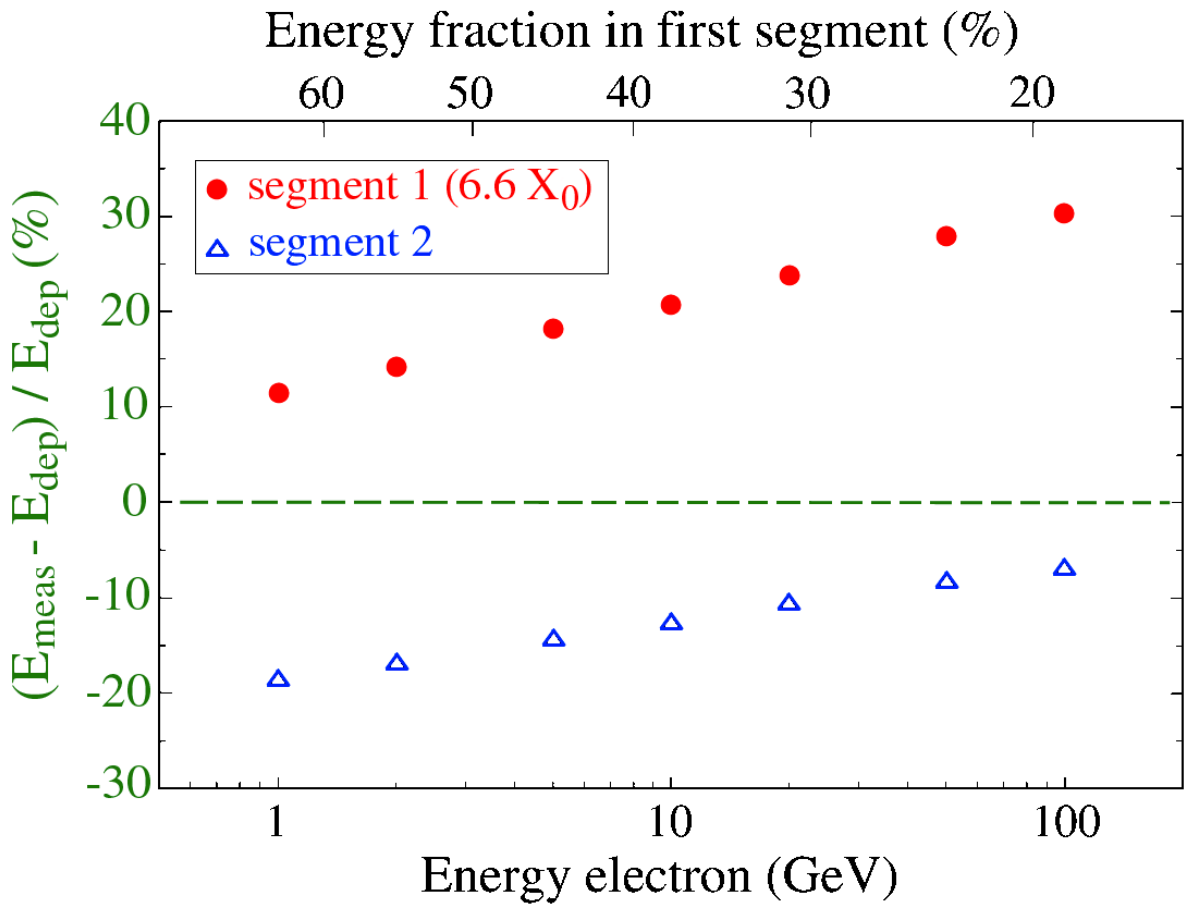

FIG. 6.3. Fractional mismeasurement of the energy deposited in the individual sections of a longitudinally segmented uranium/plastic-scintillator calorimeter, as a function of the energy of the showering electrons (bottom axis) or the energy sharing between the two calorimeter sections (top axis). The energy in the first, $6.6X_0$ deep section is systematically overestimated, the energy in the second segment is systematically underestimated, when the scintillator signals are considered a measure for the deposited energy.

Calibration by Minimizing Total Width

- Calibration methods based on minimizing total width are affected:
  - Calibration constants are energy dependent
  - Response non-linearity is introduced
  - Systematic mismeasurement of energy
    ($e.g.$, π^0, e and γ of same energy give different measurement results)

Calibrating longitudinally segmented calorimeters

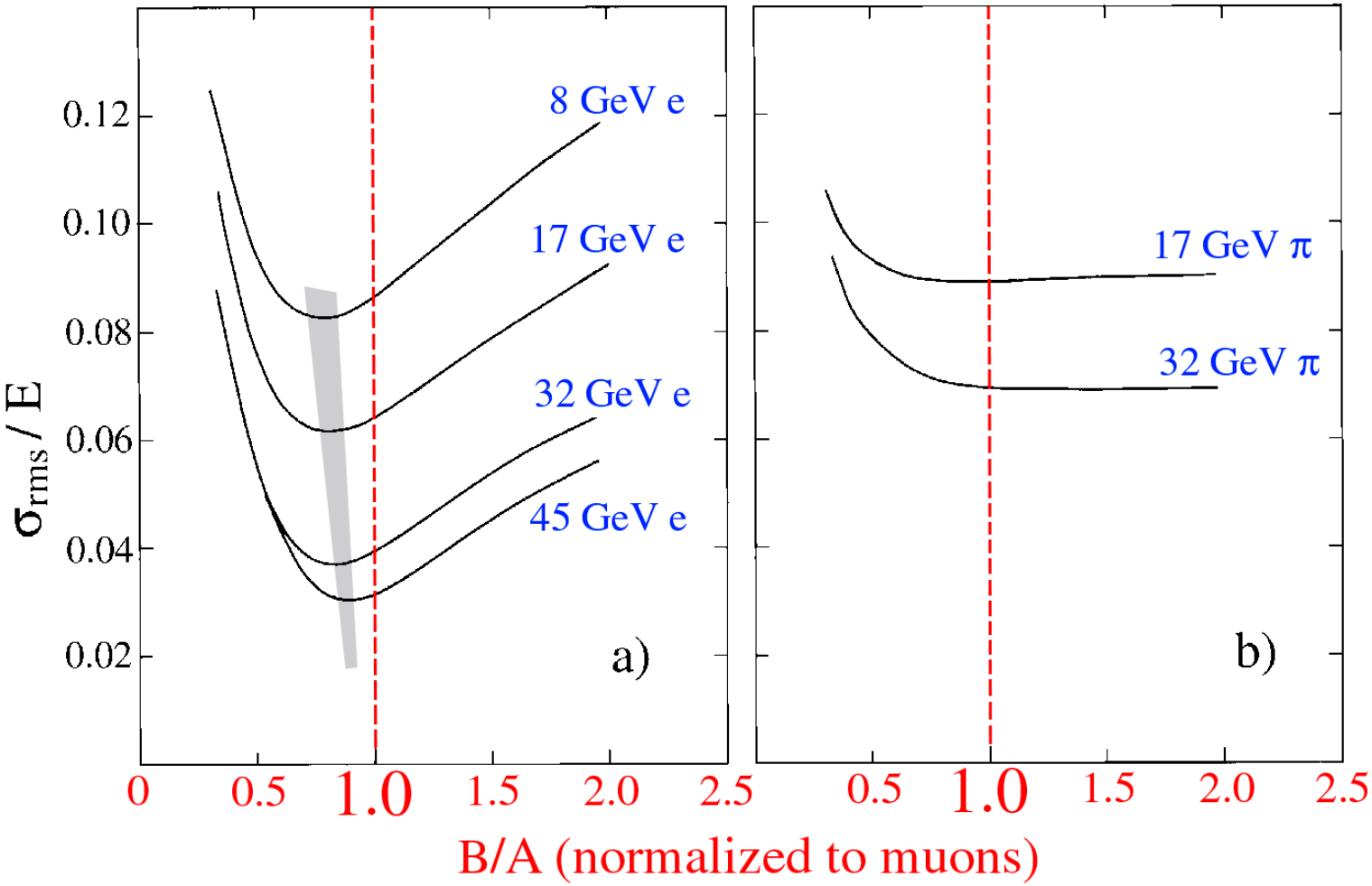

FIG. 6.2. The fractional width σ/E of the signal distributions for electrons (a) and pions (b) of different energies, as a function of the value of the intercalibration constant B/A of the HELIOS calorimeter system. The dashed line corresponds to the intercalibration constant derived from muon measurements [Ake 87].

Results of miscalibration: Non-linearity

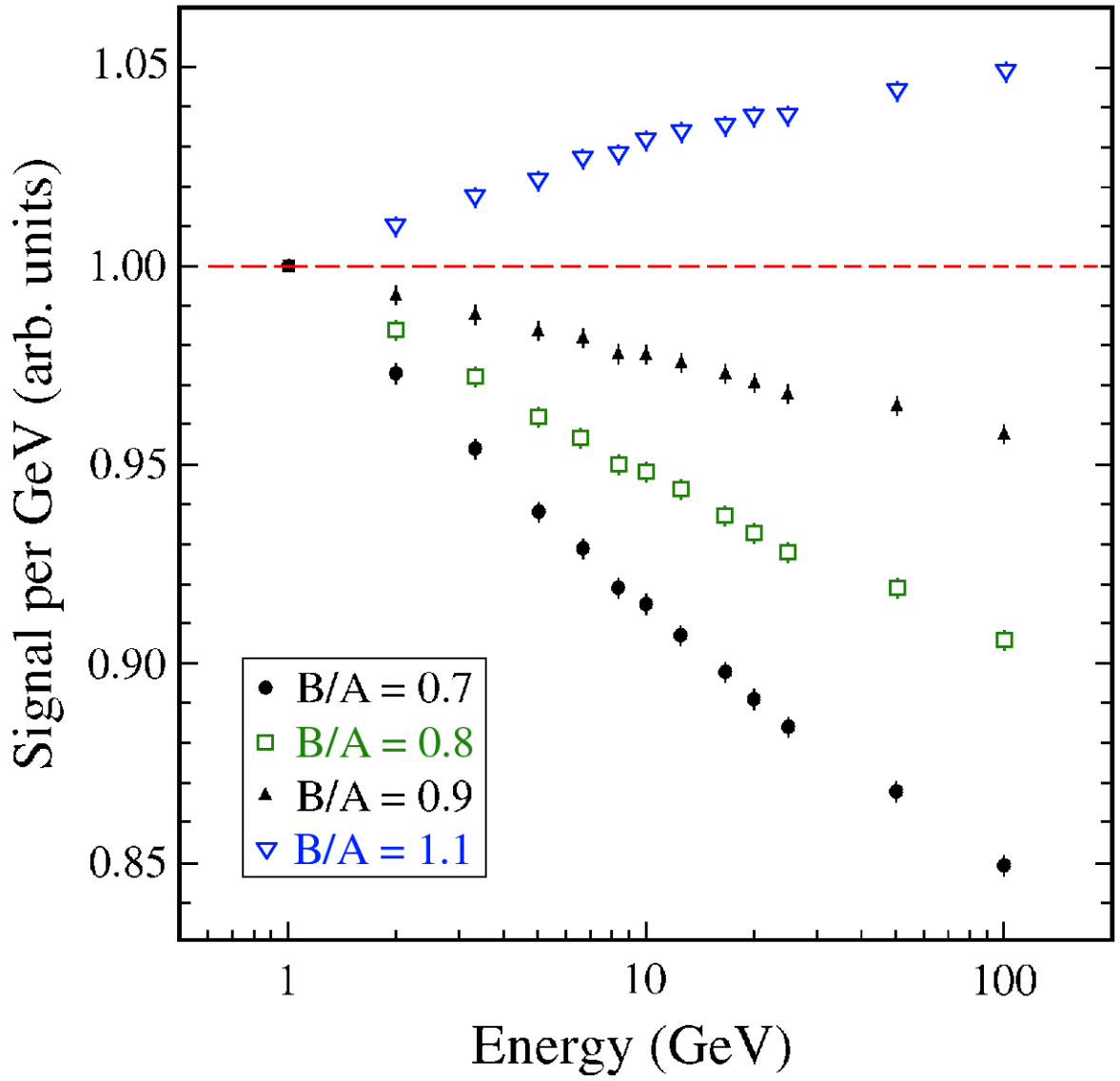

Figure 12: Signal nonlinearity for electrons resulting from miscalibration of a longitudinally segmented calorimeter. The total calorimeter response (average signal per unit of energy) is given for 3 different values of the ratio of the calibration constants for the 2 longitudinal segments, B/A. See text for details.

Results of miscalibration: Mass dependence

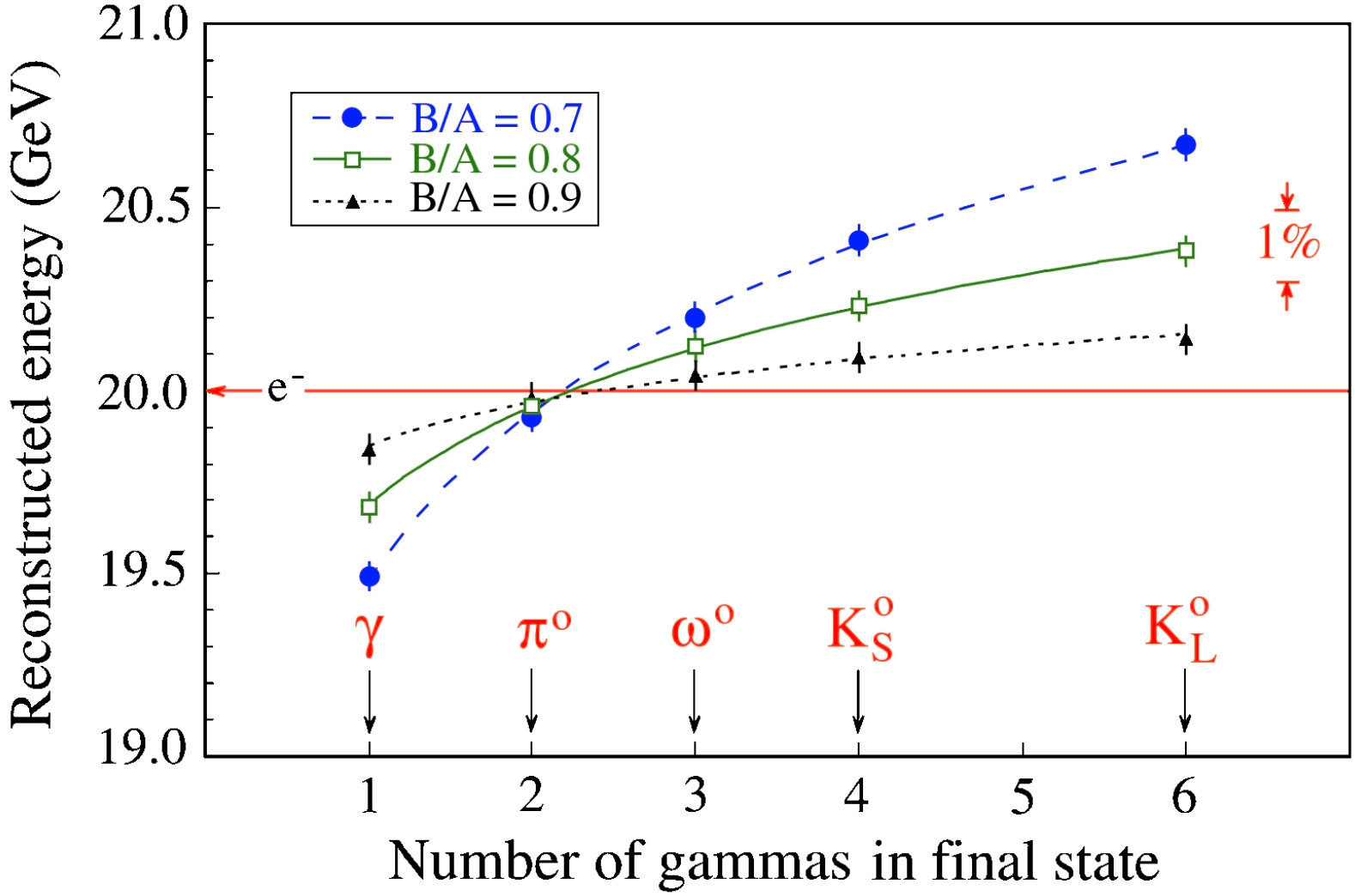

Figure 13: The average reconstructed energy for 20 GeV γs and for 20 GeV particles decaying into multiple γs in a longitudinally segmented Pb/scintillator calorimeter that was calibrated with 20 GeV electrons, for different values of the ratio of the calibration constants for the 2 longitudinal segments, B/A. See text for details.

Results of miscalibration: Mass dependence

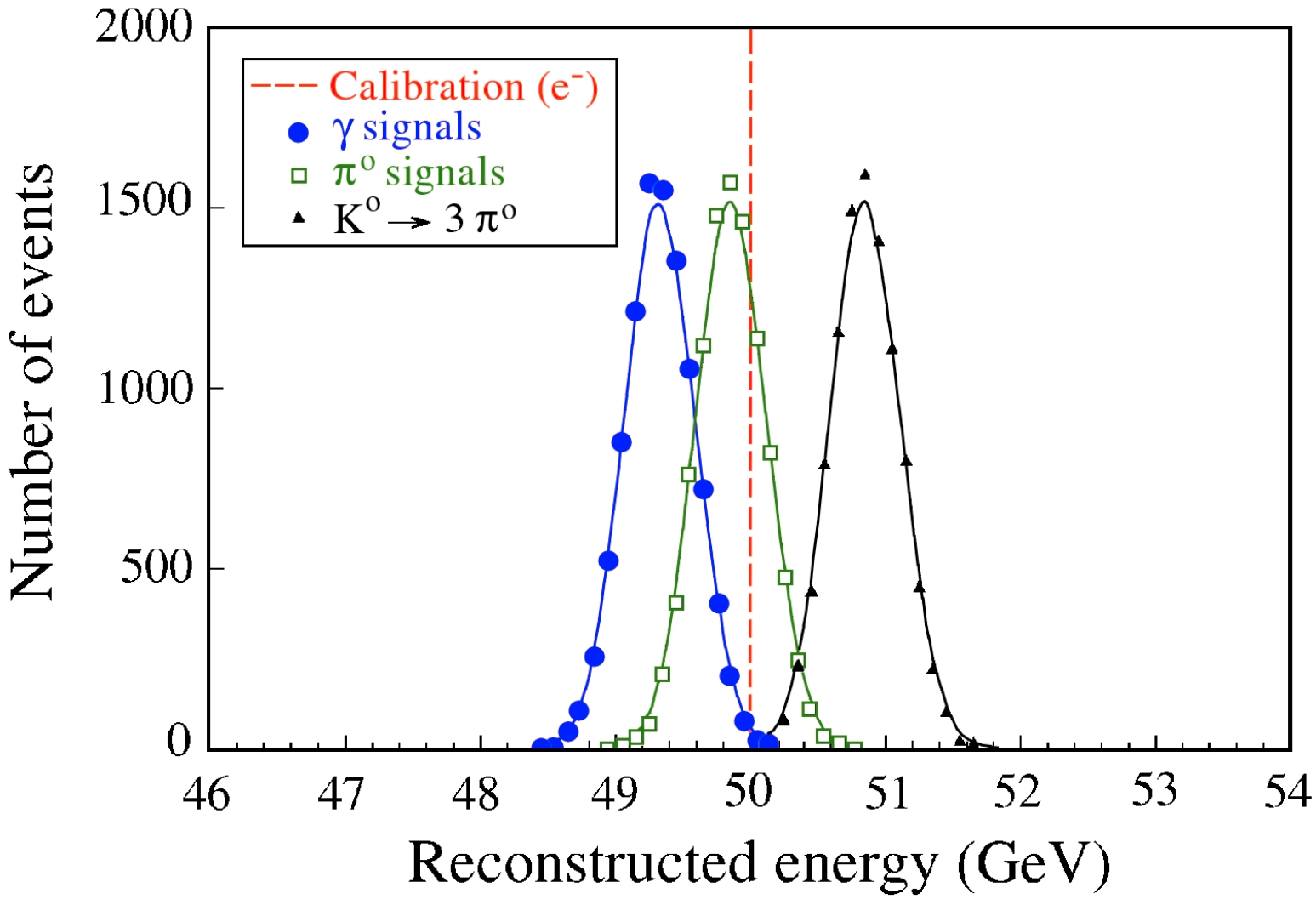

Figure 14: Signal distributions for γs and various hadrons decaying into all-γ final states. All particles have the same nominal energy and the detector, which has an intrinsic resolution of 0.5% for em showers of this energy, was calibrated with electrons using $B/A = 0.8$. See text for details.

Calibration (hadrons)

- Effects are even *worse for hadrons*
  - Reconstructed energy depends on starting point of shower
  - If calorimeter is calibrated with pions, jet energies are systematically mismeasured
- Resolution is not only determined by the width of a signal distribution, it is also necessary that the distribution is centered around the correct value
- For purposes of energy measurement, a non-segmented calorimeter is preferable

Calibration of hadron calorimeters

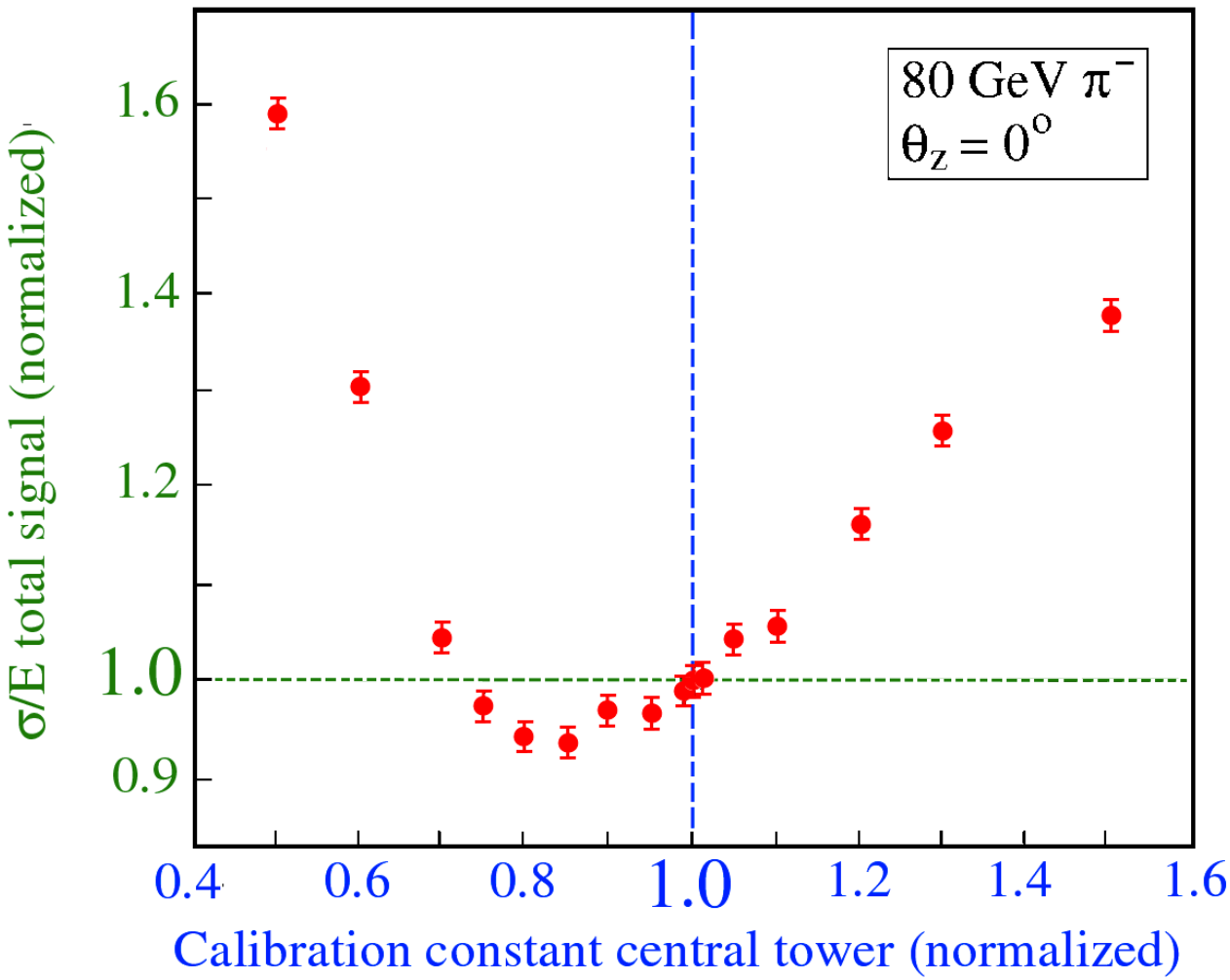

Figure 11: The fractional width, σ/E, of the signal distribution for 80 GeV π^- in the SPACAL detector as a function of the weighting factor applied to signals from the central calorimeter tower into which the pion beam was steered. The calorimeter towers were calibrated with high-energy electrons [7].

Wrong B/A: Response depends on starting point

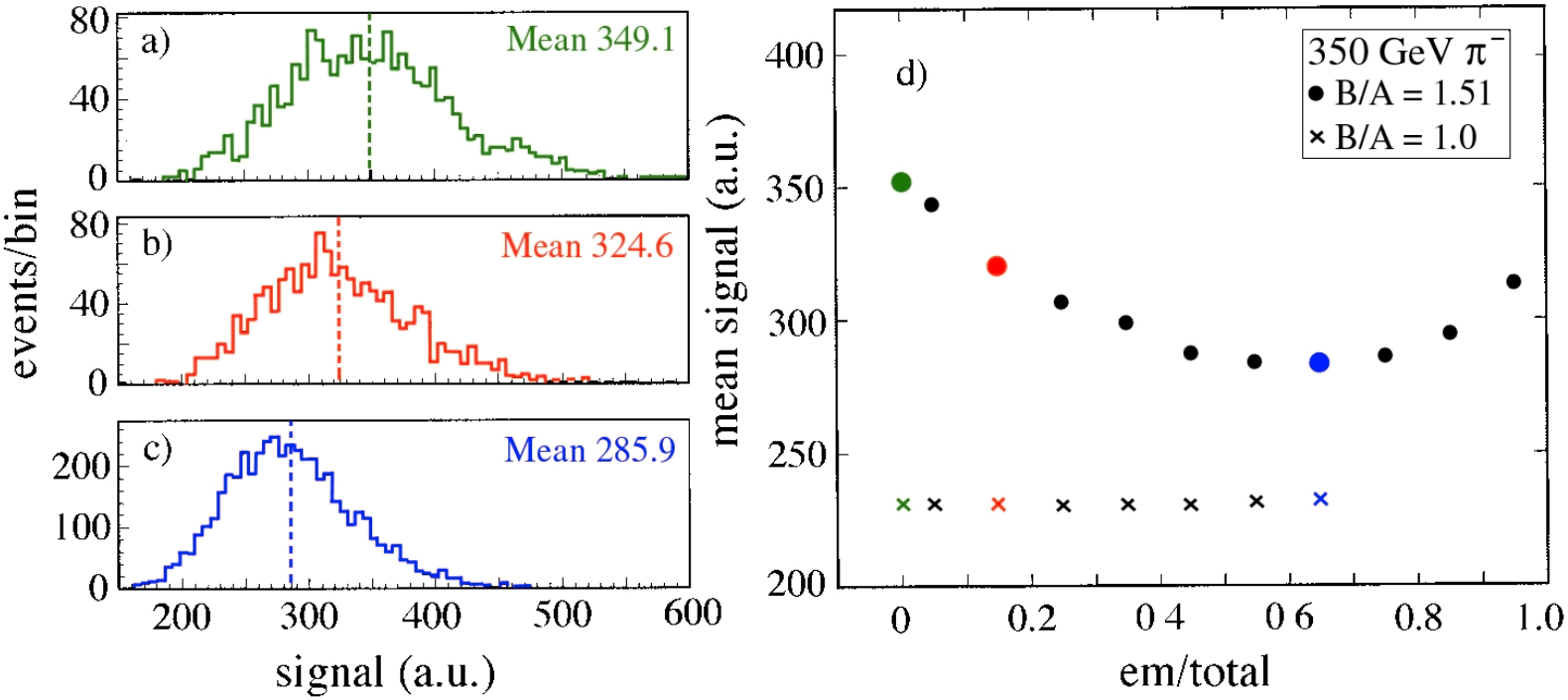

FIG. 6.10. Signal distributions for 350 GeV pion showers in a longitudinally segmented quartz-fiber calorimeter, for events in which different fractions of the (unweighted) shower energy were recorded in the em calorimeter section. Shown are distributions for which this fraction was compatible to zero (a), 10–20% (b), or 60–80% (c). The average calorimeter signal for 350 GeV pions, as a function of this fraction, is shown in diagram (d). The calorimeter was calibrated on the basis of $B/A = 1.51$ in all these cases, as required for reconstructing the energy of 350 GeV pions that penetrated the em compartment without undergoing a strong interaction. Diagram (d) also contains results (the crosses) obtained for a calorimeter calibration on the basis of $B/A = 1$. From [Gan 98].

Effects of miscalibration: Mass reconstruction

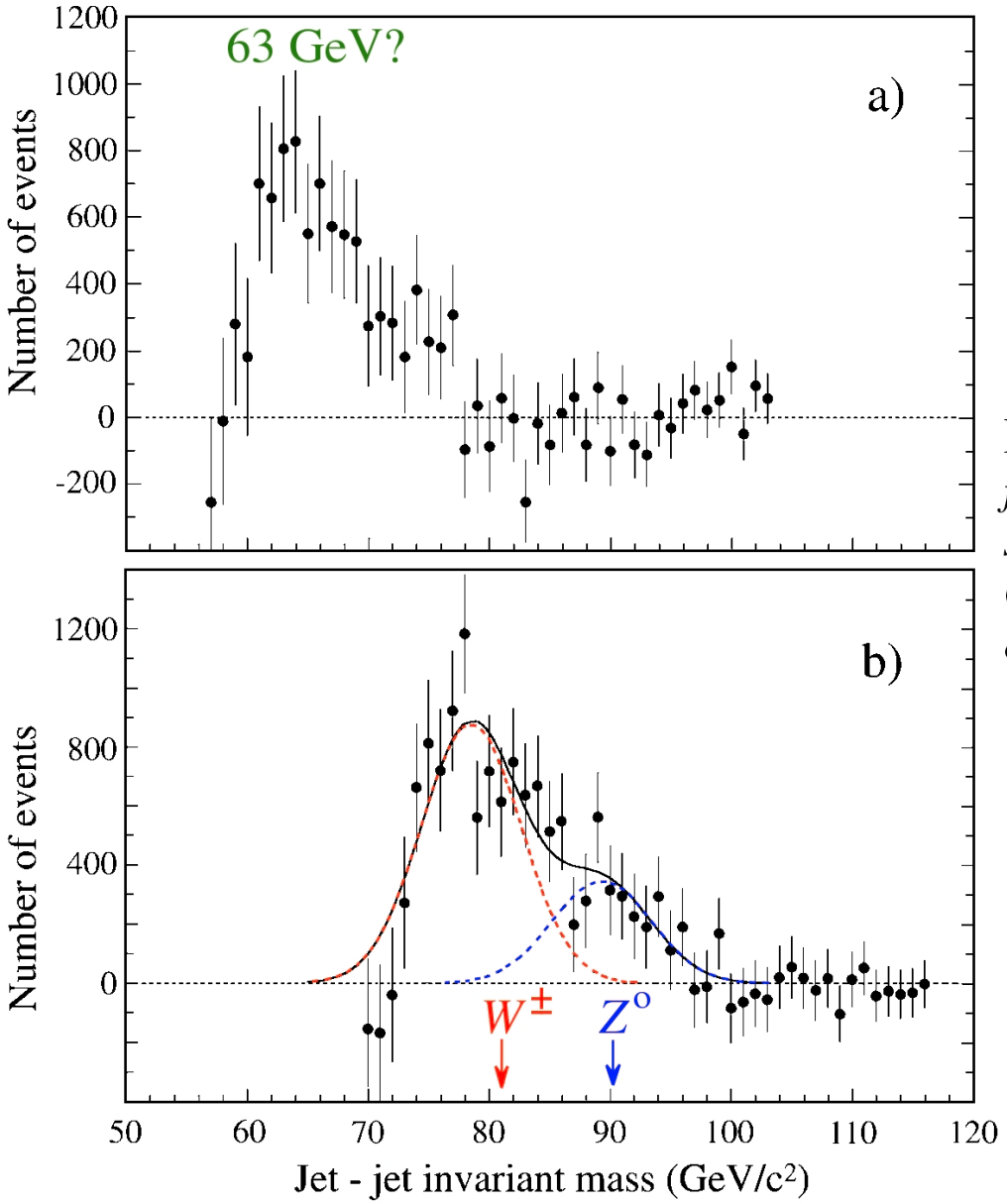

Figure 2.27: *The jet-jet invariant mass distribution for CDF Run Ic. The background has been subtracted. Results are shown for the standard CDF calbration constants* (a) *and for our alternative calibration scheme* (b).

Monte Carlo simulations and calorimetry

- *Electromagnetic calorimetry*

  EGS4 highly reliable $\rightarrow$ learned a lot of important things

  - Origin of $e/mip \neq 1$, Z-dependence of effect
  - Detailed understanding of sampling fluctuations
  - Cause of depth dependence of sampling fraction
  - Angular response dependence of fiber calorimeters
  - *etc.*

Monte Carlo simulations and hadron calorimetry

- *Hadron calorimetry*

  GEANT/GEISHA/FLUKA .... *have not contributed anything* to our fundamental understanding of hadron calorimetry

  Progress in understanding has been made *despite* these programs

  Simulations are *flawed at fundamental levels*, *e.g.* π^0 production and neutron contributions to the signals, which are crucial for understanding hadron calorimetry

  Benchmark data for tests of MC simulations:

- E. Bernardi *et al.*, NIM **A262** (1987) 229
- G. d'Agostini *et al.*, NIM **A274** (1989) 134
- N. Akchurin *et al.*, NIM **A408** (1998) 380.

Benchmark data for hadronic Monte Carlo

Test of π^0 production modelling

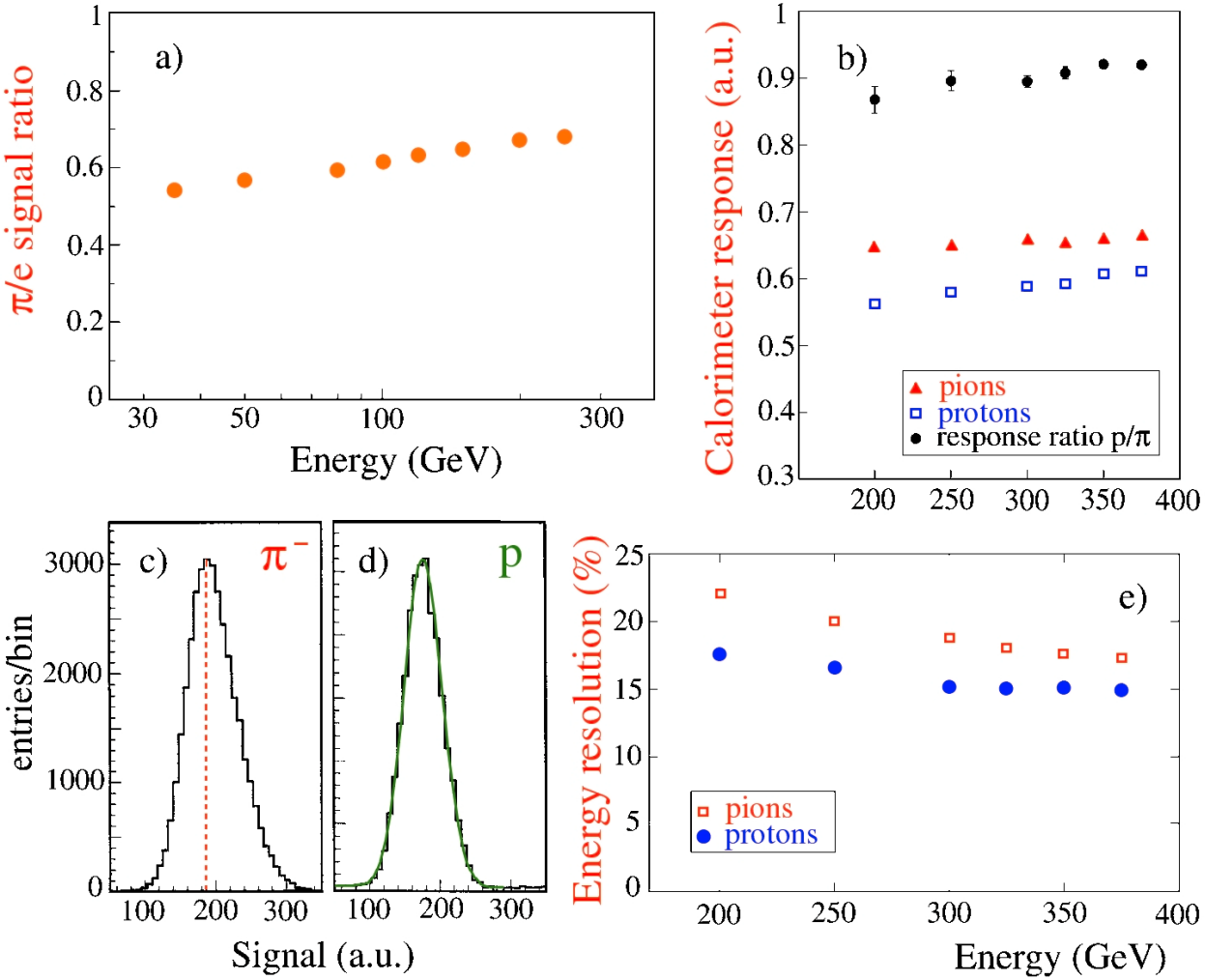

FIG. 8.27. Calorimeter benchmark data for testing the correct implementation of π^0 production in Monte Carlo simulations of hadronic shower development. Experimental data from a copper/quartz-fiber calorimeter, showing the π/e signal ratio as a function of energy (a), the response to protons and pions, as well as the ratio of these responses, as a function of energy (b), the response functions to 300 GeV pions (c) and protons (d), and the energy resolutions for pions and protons as a function of energy (e) [Akc 97].

Benchmark data for hadronic Monte Carlo

Test of description neutron effects

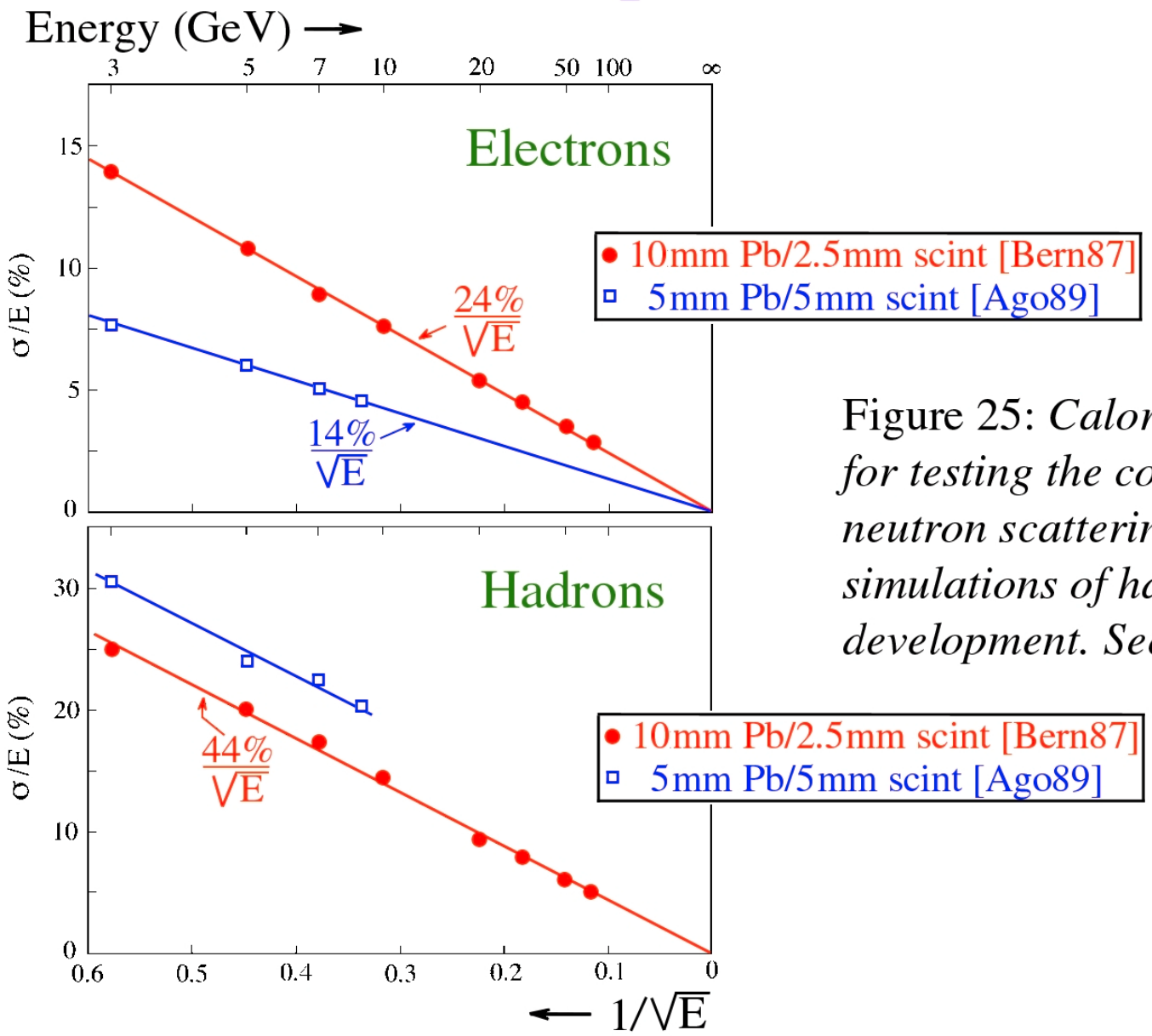

Figure 25: *Calorimeter benchmark data for testing the correct implementation of neutron scattering data in Monte Carlo simulations of hadronic shower development. See text for details.*